

Multifunctional Liquid Crystal Device for Grayscale Pattern Display and Holography with Tunable Spectral-Response

Kuixian Chen, Chunting Xu, Zhou Zhou, Zile Li,* Peng Chen,* Guoxing Zheng,* Wei Hu, and Yanqing Lu

Conventional liquid-crystal (LC) devices can only realize a single-manipulation of optical amplitude or phase, which hinders the development of LC devices toward ultracompact multifunctional integration. Herein, it is shown LC devices can be readily extended to multifunctional ones without the cost of complex design and fabrication. Specifically, by combining Pancharatnam–Berry phase with orientation-degeneracy implied in Malus's law, each operation-unit of LC devices can manipulate the amplitude and phase of incident light separately, representing a new paradigm for designing innovative LC devices. A multifunctional LC device which can display a grayscale pattern right at the surface of LC, while simultaneously project an independent phase-only holographic image in the far-field is experimentally demonstrated. More interestingly, with the LC directors tilted with external applied voltages, a new degree-of-freedom is provided to modulate the spectral-response of LC devices, contributing to the distinct function of optical switch. Owing to these unique characteristics of dual-manipulations and spectrum-tunability, the proposed multifunctional LCs have promising prospects in information multiplexing, optical communications, spectral measurements, etc.

1. Introduction

Liquid crystals (LCs), with the unique optical characteristics of polarization control and sensitivity to external-stimuli response, have been widely used in displays,^[1–5] optical communications,^[6,7] biosensing,^[8–11] and spatial light modulations.^[12–17] Owing to the specific state of matter in LCs, external electric field can be employed to modulate the orientations of LC directors, resulting in the change of anisotropy and forming pixels with different optical amplitude/intensity, which is also known as the electro-optic effects of LCs.^[18] Except for intensity modulation, the phase modulation in LCs is usually derived from the optical path differences and depends on the thickness of the LC layer. Recently, originating from the spin–orbit interaction of light in inhomogeneous anisotropic media, continuous phase modulation can be achieved in LCs via the Pancharatnam–Berry (PB) phase.^[19]

On the other hand, LCs not only perform well in the visible light band, but also exhibit excellent electro-optic characteristics in the infrared band,^{[20][21]} and even longer-wavelength terahertz band.^[22–24] Therefore, LCs are widespread in information optics and adaptive optics.^[25–30] However, due to the limited degree-of-freedom, it is difficult to manipulate amplitude and phase of light separately via a single LC device, which greatly hinders LC devices toward ultracompactness, flexibility, and multifunctionality.


In this work, we propose a design scheme of LCs which can separately manipulate optical intensity and phase to achieve information-multiplexing by reconfiguring the in-plane orientation angles of LC operation-units. Specifically, a multifunctional LC device is demonstrated to build two independent information channels for recording two different images (a grayscale pattern right at the LC surface and a holographic image in the far-field), enabled by Malus-law-assisted intensity modulation and PB phase modulation, respectively. It should be noted that our multifunctional LC device is not based on segmented or interleaved design approaches which would lower down the pixel-resolution and cause crosstalk. Instead, each LC operation-unit in our design can manipulate the optical intensity and phase separately. Therefore, our strategy paves a

K. Chen, Z. Zhou, Z. Li, G. Zheng
Electronic Information School
Wuhan University
Wuhan 430072, China
E-mail: lizile@whu.edu.cn; gxzheng@whu.edu.cn

C. Xu, P. Chen, W. Hu, Y. Lu
National Laboratory of Solid State Microstructures
Key Laboratory of Intelligent Optical Sensing and Manipulation, and
College of Engineering and Applied Sciences
Nanjing University
Nanjing 210093, China
E-mail: chenpeng@nju.edu.cn

Z. Li, G. Zheng
Peng Cheng Laboratory
Shenzhen 518055, China

Z. Li
Suzhou Institute of Wuhan University
Suzhou 215123, China

 The ORCID identification number(s) for the author(s) of this article can be found under <https://doi.org/10.1002/lpor.202100591>

DOI: 10.1002/lpor.202100591

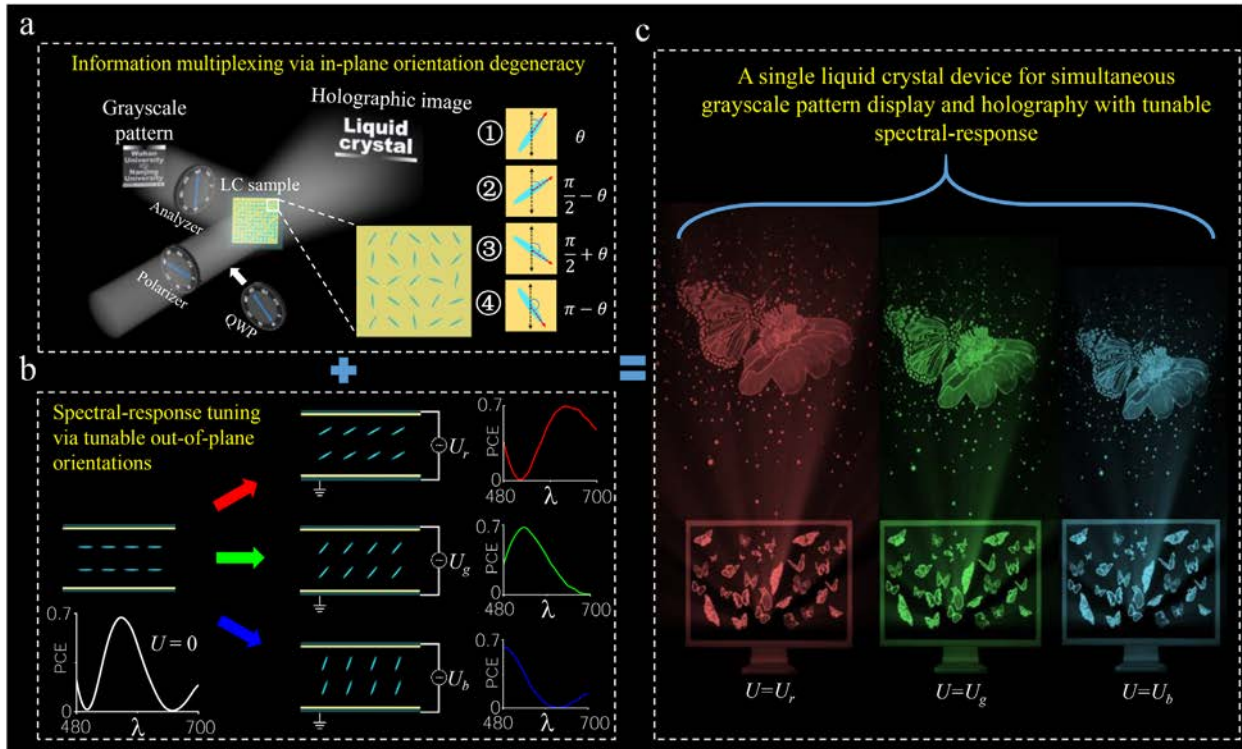


Figure 1. Operation schematics of the multifunctional LC device for simultaneous grayscale pattern display and holography with tunable spectral-response. a) Working principle illustration of information multiplexing via in-plane orientation degeneracy. As shown in the right-bottom, there are four orientation options of the LC directors to produce equal light intensity but four different PB phase delays. Hence, each LC director with a fixed in-plane orientation angle contains independent information from a grayscale pattern displayer (enabled by light intensity modulation) and a hologram (enabled by PB phase), which can be decoded by two different optical setups: a collaboration of a polarizer and an analyzer with orthogonal-polarization directions to decode the grayscale pattern right at the LC surface; a collaboration of a polarizer and a quarter-wave plate (QWP) to generate circularly polarized light to decode the holographic image in the far-field. b) Spectral-response tunability via out-of-plane orientations. With different applied voltages, the polarization-conversion efficiency (PCE) and the spectral response of the multifunctional LC device varies with out-of-plane tilting of LC directors. Here λ represents wavelength with a unit of nanometer. c) Schematic illustration of the multifunctional LC device with spectral-response tuned by applying three different external voltages U_r , U_g , and U_b , respectively.

minimalist way for information multiplexing without increasing the complexity of both design and fabrication. More interestingly, we find that by applying external voltages, each LC director can tilt from the state of in-plane to out-of-plane, and the out-of-plane orientation angles vary with the increase of applied voltages, which does not affect the in-plane operation of LCs but provides a new degree-of-freedom to modulate the spectral response and contributes to the function of optical switch.

The basic concept for the dual manipulations is presented in **Figure 1a**, where two independent images are presented right at the LC surface and in the far-field, respectively. Additionally, as shown in **Figure 1b**, the out-of-plane orientation angles of LC directors are dynamically controlled with the applied voltages, leading to a variation of spectral response. Hence, an electrically tunable multifunctional LC device for separately displaying a grayscale pattern and a holographic image can be established, as shown in **Figure 1c**. The proposed LC device, featuring dual manipulations, efficient information multiplexing, spectrum-tunability, and external field sensitivity, has promising application prospects in many potential fields, including information multiplexing, optical communications, augmented/virtual reality, and so on.

2. Working Principle and Design of the Multifunctional LC Device

The schematic configurations of the multifunctional LC operation-unit cell without and with an external voltage are presented in **Figure 2a,b**, respectively. The zoom-in-view in **Figure 2a,b** shows a LC director with both an in-plane orientation angle (θ) and an out-of-plane orientation angle (α). The LC cell, a birefringent structure, consists of five layers: upper indium-tin-oxide (ITO) glass, upper photoalignment layer,^[19] nematic LC (NLC) layer, lower photoalignment layer, and lower ITO glass. For linearly polarized (LP) incident light, the transmitted light intensity I which follows the Malus law, can be expressed as

$$I = I_0 \sin^2(2\theta) \left| \frac{1 - e^{i\delta}}{2} \right|^2 \quad (1)$$

where I_0 is the incident light intensity, δ is the phase retardation between two orthogonally-polarized light along the ordinary and extraordinary axes, which can be written as

$$\delta = \frac{2\pi(n_e - n_o)d}{\lambda} \quad (2)$$

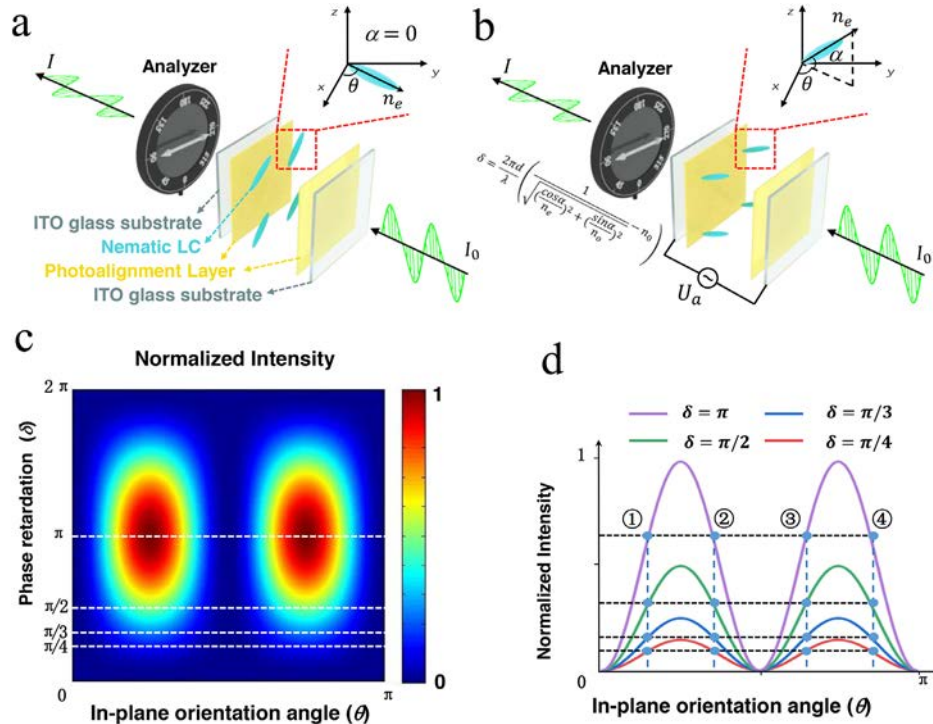


Figure 2. Working principle of the electrically tunable LC device. a) Schematic configuration of intensity manipulation without applied voltages. θ and α represent the in-plane and out-of-plane orientation angles of the LC operation-unit, respectively. The phase retardation (δ) maintains constant without applied voltages. The incident light propagates along the z -axis. b) Schematic configuration of intensity manipulation with applied voltages. The LC directors tilt from in-plane to out-of-plane with applied voltages, and the change of out-of-plane orientation angle results in the variation of phase retardation, and then optical intensity. c) Normalized optical intensity with different in-plane orientation angle and phase retardation. d) Transversal interception line of c) show that there are four orientation angles (θ , $\pi/2-\theta$, $\pi/2+\theta$, $\pi-\theta$) corresponding to an equal optical intensity for LP light incidence but different PB phase with circularly polarized (CP) light incidence.

In Equation (2), n_o and n_e denote the refractive index along the ordinary and extraordinary axes, respectively, λ is the wavelength of the incident light, and d is the thickness of the NLC layer. As the in-plane orientation angle (θ) varies, the transmitted light intensity can reach its maximum $I_0 |\frac{1-e^{i\delta}}{2}|^2$, and $|\frac{1-e^{i\delta}}{2}|^2$ corresponds to the PCE of the LC with the LP light incidence. Meanwhile, as for the incidence of CP light, PCE of the LC is the ratio of the transmitted light intensity carrying the additional phase to that of the incident light intensity, which also equals to $|\frac{1-e^{i\delta}}{2}|^2$ as demonstrated in Note S1 (Supporting Information). Moreover, the additional phase of the transmitted CP light with opposite helicity is $\psi = \pm 2\theta$ (positive sign for left-handed CP incident light, while negative for right-handed CP), known as the PB phase.^[19] The PB phase has been employed in LC devices to realize arbitrary wavefront engineering, such as spin-controlled focus/defocus and vortex/vector beam generation.

Furthermore, by applying external electric field to the LC director, the anisotropy axis of the LC director will be switched from in-plane to out-of-plane, causing a variation of anisotropy. Along with the tilting, the effective refractive index of the extraordinary axis can be calculated by

$$n_{\text{eff}} = \frac{1}{\sqrt{\left(\frac{\cos\alpha}{n_e}\right)^2 + \left(\frac{\sin\alpha}{n_o}\right)^2}} \quad (3)$$

where α represents the out-of-plane orientation angle of the LC director. With an increasing applied voltage, α can vary from 0 to $\pi/2$, causing the change of n_{eff} from n_e to n_o .^[31] For a certain wavelength λ , the phase retardation can be re-expressed as

$$\delta = \frac{2\pi (n_{\text{eff}} - n_o) d}{\lambda} \quad (4)$$

Thanks to the varied anisotropic refractive index, we can endow the LC directors with electrically tunable phase retardations for a given thickness and certain wavelength, as shown in Figure 2b. By modulating the out-of-plane orientation angles of the LC device with different external electric fields, one can realize the dynamic tunability of PCE from 0 to 1, leading to the function of optical switch.^[32] Figure 2c shows intensity manipulation can be achieved via the in-plane and out-of-plane orientation angles of LC directors.

Interestingly, as illustrated in Figure 2d, there is a one-to-four mapping relationship in LC directors between the optical intensity and the in-plane orientation angle, which can be employed to design multifunctional LC devices. Particularly, the four in-plane orientation angles (θ , $\pi/2-\theta$, $\pi/2+\theta$ and $\pi-\theta$), which have been illustrated in Figure 1a, correspond to an equal transmitted light intensity for LP light incidence but different PB phases of 2θ , $\pi-2\theta$, $\pi+2\theta$, and $2\pi-2\theta$ for left-handed CP incident light. This interesting physics can be called orientation degeneracy,

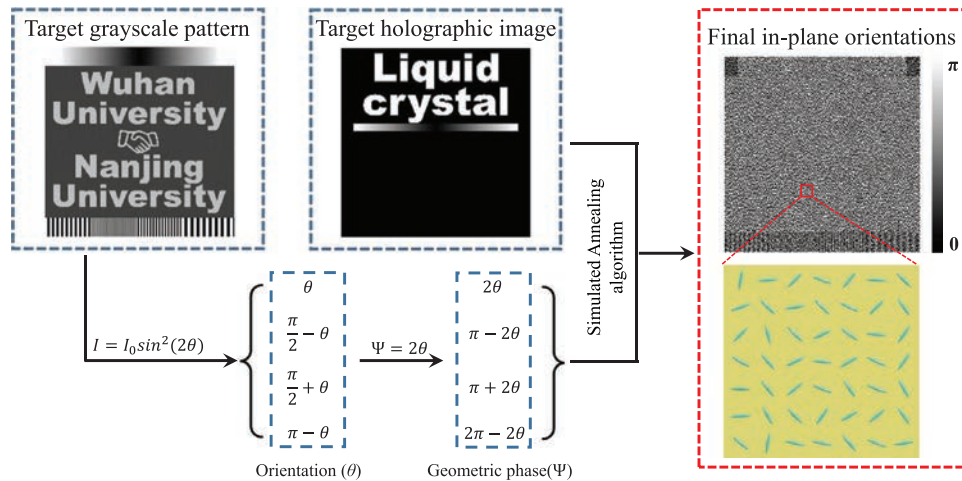


Figure 3. Design process of the multifunctional LC device. Design flowchart of the multifunctional LC device to simultaneously encode a grayscale pattern and a four-step phase-only holographic image. The grayscale pattern and the holographic image are both composed of 250×250 pixels, and the final in-plane orientation angle distribution is shown in the right side.

i.e., different orientation angles correspond to the same optical intensity, which is similar with the concept designed with anisotropic nanostructures in metasurface community.^[33–35] Therefore, with the design degree-of-freedom gifted by orientation degeneracy of LC directors, we can obtain not only continuous intensity modulation but also simultaneous four-step phase manipulation with each LC operation-unit, thus forming two independent information channels without the cost of complex design and fabrication.

Next, we show how to encode two independent information into the in-plane orientation angles of the LCs. As shown in **Figure 3**, based on the relationship between the transmitted intensity I and the in-plane orientation angle θ indicated by Equation (1), we encode the optical intensity of the target grayscale pattern in the in-plane orientation angles of the LCs. For each unit-cell, the in-plane orientation of LC director has four options owing to the one-to-four mapping relationship between optical intensity and orientation angle, and can possess different geometric phases. Here, according to the target holographic image, we employ the simulated annealing algorithm^[36] to determine the in-plane orientation angle in four options, and the final in-plane orientation angle distribution is shown in **Figure 3** (more details about phase optimization with simulated annealing algorithm are presented in Note S2, Supporting Information).

In the multifunctional LC design, we not only encode the information of a grayscale pattern and a holographic image into LC operation-units with different in-plane orientation angles, but also select the optimal operating wavelength by tilting their out-of-plane orientation angles with different applied voltages. To realize the above design in the LC cell, we make use of a photoalignment technique based on a home-made dynamic microlithography system. Here, a polarization-sensitive and rewritable alignment agent is adopted,^[37] which has shown great potentials for arbitrary and precise LC patterning.^[16] Processing details are provided in the Experimental Section. The inset of **Figure 4a** exhibits the multifunctional LC device composed of 250×250 working units corresponding to the orientation angle distribution shown in **Figure 3**. It looks transparent without the polarizer or analyzer.

Each working unit-cell has dimensions of $20 \times 20 \mu\text{m}^2$, and the thickness of LC cell is $6 \mu\text{m}$ in our experiment. To simplify the sample fabrication, the in-plane orientation angles of the multifunctional LC were 36-step quantified equidistantly and the quantification errors are analyzed in Note S4 (Supporting Information), which verifies the robustness in the design of electrically tunable wave plate.

3. Experimental Results of the Multifunctional LC Device

Without applied external voltage, the experimentally measured PCE of the LC device is presented in **Figure 4a**, which is measured by the optical setups shown in Note S5 (Supporting Information). As shown in the curve, the PCE floats with the wavelength rising from 480 to 700 nm, and reaches its maximum at 560 nm. Then we employ the optical setup illustrated in Note S6 (Supporting Information) to observe the grayscale pattern decoded at the LC surface. The LC device is illuminated by a white light source with different orthogonal-polarization combination of the polarizer and the analyzer, and the experimentally captured grayscale patterns are presented in **Figure 4b**. When the transmission axis of the polarizer is parallel to the x -axis, we can clearly observe that the grayscale pattern illustrated in the left side of **Figure 4b** is consistent with the target picture, which indicates that the LC device works well for the intensity modulation right at the LC surface. Although the fabrication errors bring some noisy speckles to the grayscale pattern, the information at the LC surface is still clearly distinguished. Besides, by rotating the transmission axis of the polarizer, the brightness of the experimental result at $\pi/4$ is complementary to that of 0, while the grayscale pattern is nearly lost in the background noise at $\pi/8$ (more details about how the polarization direction affects the grayscale pattern can be found in Note S7, Supporting Information).

Since the varied wavelength leads to a continuous change of the PCE in **Figure 4a**, we further explore the influence of wavelength on performance, and the experimentally captured patterns are presented in Note S6 (Supporting Information). The target

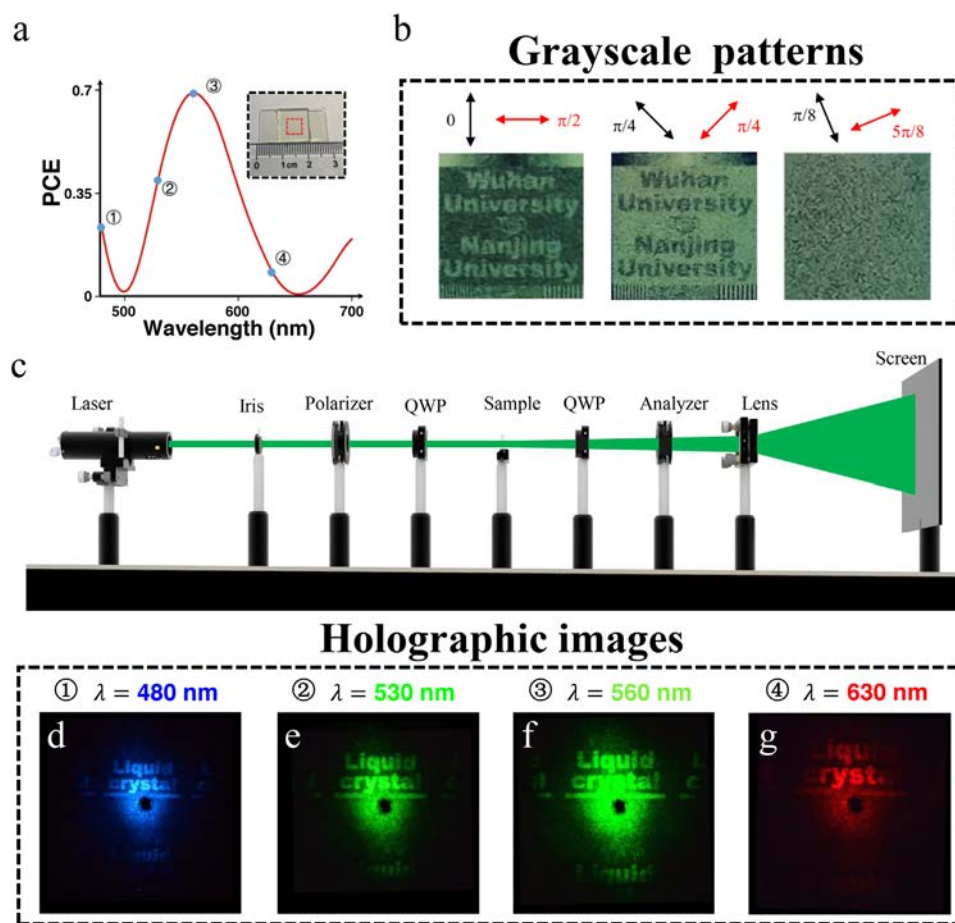


Figure 4. Experimental results of the multifunctional LC device without applied voltage. a) PCE of the LC device for different wavelengths. The inset picture exhibits the multifunctional LC device and the red marked box indicates the working area. b) Experimentally captured patterns of the working area illuminated by a white light source with different orthogonal-polarization combination of the polarizer and the analyzer. The black and red arrows represent the transmission axis directions of the polarizer and analyzer, respectively. c) Optical setup for observing holographic image in the far-field. d–g) Experimentally captured holographic images at four different wavelengths ($\lambda = 480, 530, 560,$ and 630 nm), captured by a commercial visible camera. The optical power of the incident laser beam is 0.5 mW. To better capture the holographic images, we dug a hole in the middle of the screen to filter the unwanted zero-order light.

information can be clearly recognized in all captured patterns, which presents the broadband response characteristic of the multifunctional LC device with respect to its functionality of displaying grayscale patterns.

Next, for the generation and observation of far-field holographic image, a different optical setup is introduced, where the LC device is illuminated by a super-continuum laser source, as shown in Figure 4c. There are two pairs of polarizer and quarter-wave plate in the holographic optical setup. The first pair is employed to convert the polarization state of incident laser beam into circular polarization, and the latter plays the role of an optical filter which only lets the cross-polarized CP light pass. Moreover, we insert a biconvex lens ($f = 40$ cm) after the analyzer to focus the holographic image at its focal plane. Figure 4d–g exhibits four far-field holographic images at four different operating wavelengths of 480, 530, 560, and 630 nm. The holographic efficiency, defined as the ratio of the transmitted energy reconstructing the holographic image to the incident light energy, is measured as 18.5%, 29.6%, 51.3%, and 6.8%, respectively (exper-

imental setup for holographic efficiency measurement is shown in Note S8, Supporting Information). All these experimental results agree well with the target holographic images but with different brightness. The brightest one and the darkest one appear at 560 and 630 nm, matching the maximum and minimum of the PCE in the picked four wavelengths, respectively (shown in Figure 4a). Therefore, according to all aforementioned experimental results, the multifunctional LC device can achieve separate manipulation of optical intensity and phase.

For further characterizing the spectral response of the multifunctional LC device with different applied voltages, we employ a commercial signal generator to offer the external electric field and measure the corresponding PCE. Figure 5a illustrates the experimental results of the PCE under the applied voltage ranging from 0 to 5 V, and there exists a threshold voltage U_0 . When the applied voltage U_a is smaller than U_0 , the PCE remains unchanged. After that, the continuously increased voltage results in the change of the PCE, which suggests the potential of tunable spectral-response. As presented in the color map of Figure 5a,

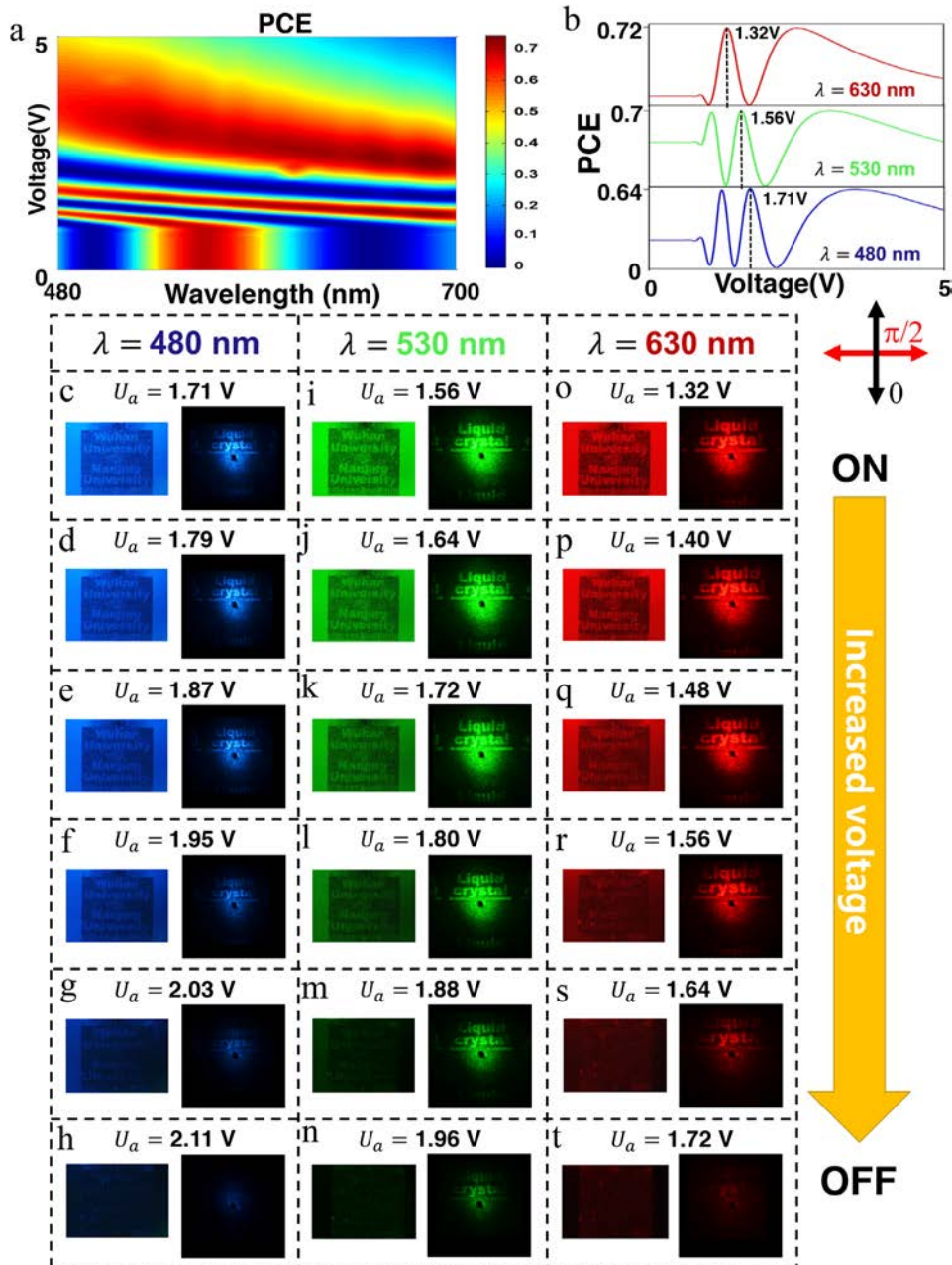


Figure 5. Spectral response of the multifunctional LC device with different external electric field. a) Measured PCE of the LC sample versus operating wavelength (ranging from 480 to 700 nm) and the applied voltages (ranging from 0 to 5 V). The threshold voltage U_0 is around 0.9 V. b) PCE of the LC device for different applied voltages. c–t) Experimental results of the grayscale pattern (left) at the LC surface and the holographic image (right) in the far-field with different applied voltages, indicating the function of optical switch from on to off. The operating wavelength is c–h) 480 nm, i–n) 530 nm, and o–t) 630 nm. The black and red arrows represent the transmission axis directions of the polarizer and analyzer in the grayscale pattern observation experimental setups, respectively. The optical power of the incident laser beam is 0.5 mW in the holographic image observation experiment.

the increase of the applied voltage results in a shift of the optimal operating wavelength. Figure 5b indicates the trend of the PCE versus the applied voltage at three operating wavelengths of 630, 530, and 480 nm, respectively, which are three special cases of the color map. Obviously, there exists an optimal match between the operating wavelength λ_0 and the applied voltage. When we increase λ_0 from 480 to 530 or 630 nm, the optimal applied voltage decreases from 1.71 to 1.56 or 1.32 V, respectively. With cor-

responding optimal applied voltages, the holographic efficiency reaches 50.9%, 54.5%, and 57.4% at the operating wavelengths of 480, 530, and 630 nm, respectively, which proves the realization of the optimal operating wavelength shift (see Movie S1, Supporting Information).

As for a certain operating wavelength, Figure 5b also shows that the PCE drops from the maximum to almost zero within a specific applied voltage range, corresponding to the switching of

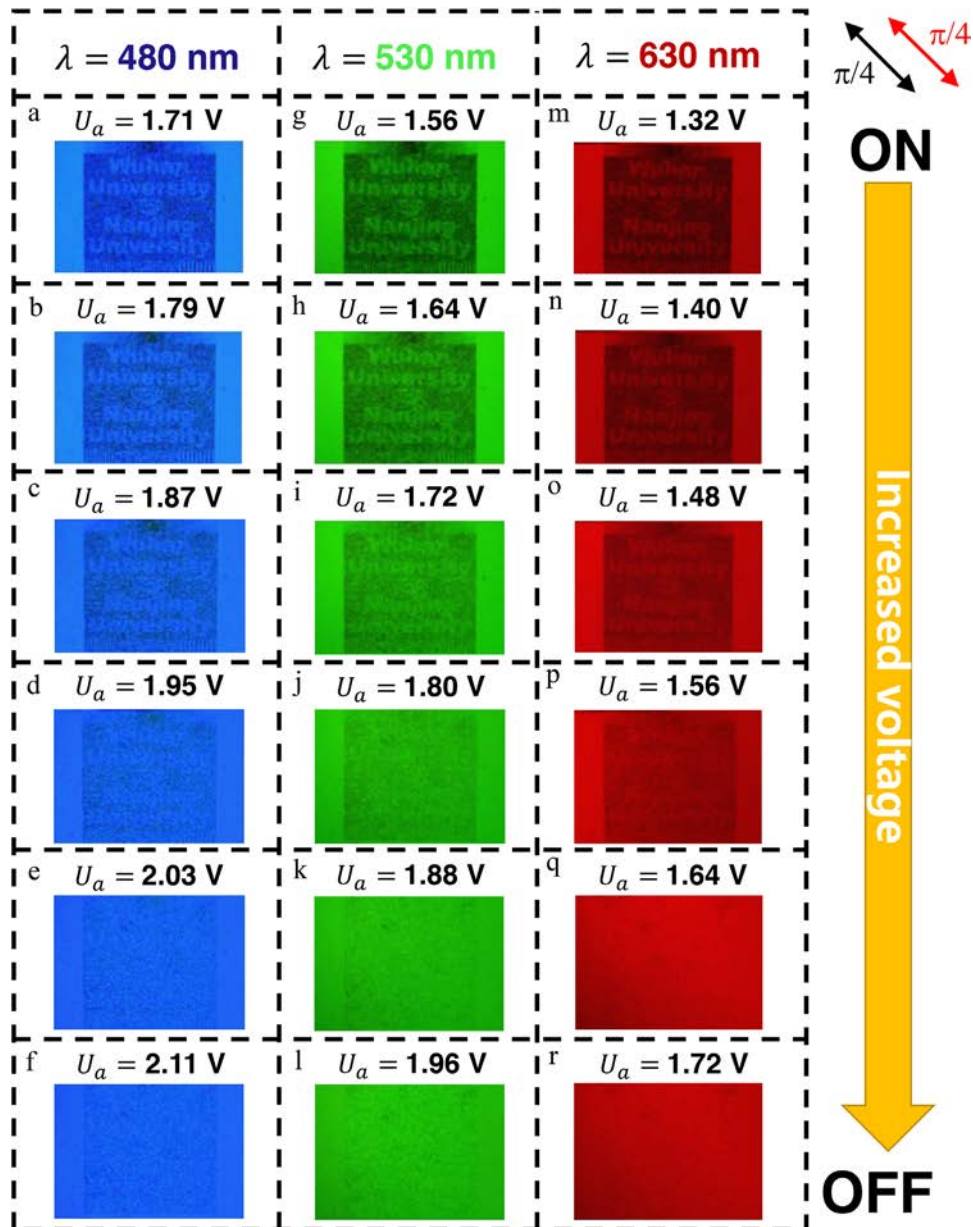


Figure 6. Experimental results of the information hiding with different external voltages and wavelengths at the LC surface. The operating wavelength is a–f) 480 nm, g–l) 530 nm, and m–r) 630 nm. The black and red arrows represent the transmission axis directions of the polarizer and analyzer in the grayscale pattern observation experimental setups, respectively.

working state from on to off (see Movie S2, Supporting Information). The switching of working states can be observed at the LC surface and in the far-field at three different wavelengths, as illustrated in Figure 5c–t. During the variation of the applied voltages, the experimental holographic efficiency in the far-field decrease and the grayscale patterns at the LC surface become darkened and finally disappear (the region outside the working area is employed for comparison here and its in-plane orientation angles are 0), which is consistent with the change of PCE.

More interestingly, the electrical tunability of spectral response can not only realize the optical switching of the working state, but also independently hide the information channel. For example,

when the transmission axes of the polarizer and the analyzer are parallel to each other of $\pi/4$, the transmitted light intensity I can be re-expressed as

$$I(\theta, \delta) = I_0 \left| \frac{1 - e^{i\delta}}{2} \sin(2\theta) + \frac{1 + e^{i\delta}}{2} \right|^2 \quad (5)$$

The contrast of the grayscale pattern reaches its maximum when the phase retardation δ is π , and the grayscale pattern only left the part unrelated to the in-plane orientation angle θ with $\delta = 0$ (more details about the equation derivation can be find in Note S7, Supporting Information). Under this circumstance, the

information channel can be independently switched from on to off by the applied voltages. As shown in **Figure 6**, the grayscale pattern at the LC surface is getting blurred with increased external voltage. The impressive electric sensitivity and tunability of spectral response endow the multifunctional LC device more potential in optical switch, inspiring a wide application prospect in optical communications, optical sensing, etc.

4. Discussion

The proposed multifunctional LC device possesses a series of unique technical characteristics over previous schemes. First, in our design, each LC operation-unit can separately manipulate the intensity and phase of the transmitted beam by reconfiguring the in-plane orientation angle. It extends the LC manipulation from conventional single-manipulation (intensity or phase) to current dual-manipulations (intensity and phase), and makes the polarization multiplexing come true without complex design and fabrication, which is hard to implement in previous LC design strategy. More detailed comparison of the proposed multifunctional LC device and related LC-based works is presented in Table S1, Supporting Information. Even if the phase cannot be arbitrarily selected, the theoretical efficiency of a four-step phase-only hologram can reach 81%, which is acceptable in the field of holography.^[38] Hence, the proposed multifunctional LC device can simultaneously play the role of displaying a grayscale pattern and a holographic image. By expanding the range of the LC in-plane orientation angle from $(0, \pi/2)$ to $(0, \pi)$, the functionality of existing commercial liquid crystal display (LCD) device is expected to be extended via the aforementioned orientation reconfiguration algorithm. Therefore, it has great potential in the field of AR/VR and information multiplexing.

Next, our proposed multifunctional LC device exhibits an impressive characteristic of spectrum-tunability. By tuning the applied voltage, the out-of-plane orientation angles vary and the in-plane orientation angles remain unchanged (i.e., the dual manipulations always work), resulting in a continuous spectral variation almost covering the visible spectra (from 480 to 700 nm). Hence, our approach possesses practical prospects in optical switching devices. Besides, due to the dependency between the spectrum and the applied voltage, our approach can also be widely employed in the field of measurement.

Last but not least, the PCE and the holographic efficiency of the proposed multifunctional LC device are relatively high (100% and 81% in theory, 73.8% and 58.4% in experiment). We notice that there are some researches of polarization multiplexing and multifunctional image display in the field of metasurfaces^[39–43] due to their ability of manipulating nanostructure's anisotropy arbitrarily.^{[44][45]} However, the dual manipulations based on LCs are first proposed here and have the advantages of adjustable spectral response, large-area manufacturing, high efficiency, and compatibility with existing commercial LCD devices. Meanwhile, the mature processing technology of the LC materials brings tremendous convenience for the mass manufacturing. These merits overcome the shortcomings of previous researches and make multifunctional LC devices more conducive to practical applications. More detailed comparison of approaches multiplexing grayscale pattern display and holography is provided in Table S2, Supporting Information.

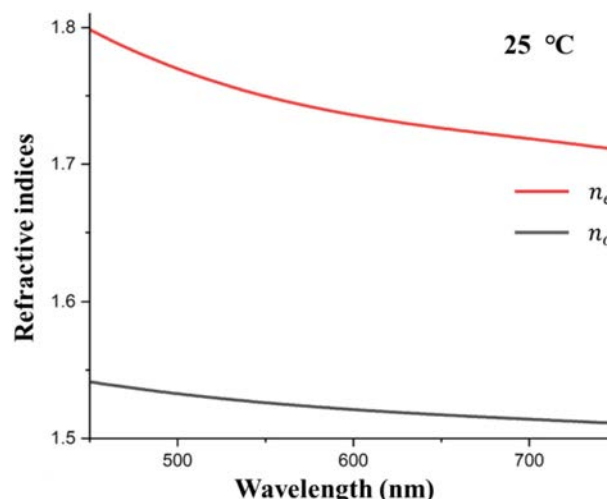


Figure 7. Anisotropic refractive indices of LCs (E7) versus wavelengths at $T = 25\text{ }^{\circ}\text{C}$.

5. Conclusion

In summary, we propose and experimentally demonstrate a multifunctional LC device to separately manipulate the intensity and phase in the visible range, forming two information channels whose spectral response is tunable by applying external voltage. Owing to the unique characteristic of orientation degeneracy of anisotropic LC operation-units, the proposed multiplexing approach retains all the advantages of LC while expanding its functionality without the cost of complex design and fabrication. With the impressive characteristics of polarization multiplexing, high efficiency, spectrum-tunability, large-area manufacturing, and easy integration with existing LCD devices, our proposed multifunctional LC device has great potential in information multiplexing, optical communications, spectral measurements, AR/VR, and many other related fields.

6. Experimental Section

Sample Fabrication: The processing is mainly divided into two parts: one is the preparation of the LC cell, and the other is the ultraviolet (UV) photopatterning technology to write the designed orientations into the LC directors (see Note S3, Supporting Information). First, ITO glass substrates were ultrasonically cleaned, UV-Ozone bathed, and then spin-coated with a 0.3% solution of the sulphonic azo-dye SD1 (Dai-Nippon Ink and Chemicals, Japan) in dimethylformamide. After curing at $100\text{ }^{\circ}\text{C}$ for 10 min, $6\text{ }\mu\text{m}$ spacers were spurted over the SD1-coated substrate and covered with the other glass substrate, forming the cell sealed with epoxy glue. For transferring the designed orientation into the SD1 layer, a DMD-based UV microlithography system which consists of a light source, a dynamic pattern generation component, an optical focusing component and a monitor is introduced. Briefly, a UV beam was reflected onto the DMD (Discovery 4195, Texas Instruments), and carried the designed pattern. Then being focused by a tunable lens, the beam was polarized by a motorized rotating polarizer and projected onto the LC cell. A charge-coupled device (CCD) was utilized to monitor the focusing process. After the nematic LCs (E7) were injected (the anisotropic refractive indices versus wavelengths are shown in **Figure 7**), the patterned SD1 can guide the orientation of the LC directors through intermolecular interactions, forming a LC cell with the designed orientations.

Characterizations: All experiments were performed at room temperature under ambient environment. All the grayscale patterns and holographic images were captured by a commercial camera (Nikon D5100). The LC sample was illuminated by a super-continuum laser source (YSL SC-pro). And the external electric field was applied by a commercial signal generator (eTBS2000X).

Supporting Information

Supporting Information is available from the Wiley Online Library or from the author.

Acknowledgements

K.X.C., C.T.X., and Z.Z. contributed equally to this work. This research was supported in part by the National Key Research and Development Program of China (Nos. 2021YFA1202000 and 2017YFA0303700), the National Natural Science Foundation of China (Nos. 91950110, 11904267, 62175101, 62035008, and 12004175), the Fundamental Research Funds for the Central Universities (Nos. 2042021kf0018 and 2042021kf1043), and the Natural Science Foundation of Jiangsu Province (No. BK20190211).

Conflict of Interest

The authors declare no conflict of interest.

Data Availability Statement

The data that support the findings of this study are available from the corresponding author upon reasonable request.

Keywords

holography, light manipulations, liquid crystals, orientation degeneracy, tunable spectral response

Received: November 5, 2021
Published online: January 23, 2022

- [1] T. J. Scheffer, J. Nehring, *Appl. Phys. Lett.* **1984**, *45*, 1021.
- [2] Y. Zhu, S. Murali, W. Cai, X. Li, J. W. Suk, J. R. Potts, R. S. Ruoff, *Adv. Mater.* **2010**, *22*, 3906.
- [3] M. Schadt, *Liq. Cryst.* **2015**, *42*, 646.
- [4] K. Srivastava, W. Zhang, J. Schneider, J. E. Halpert, A. L. Rogach, *Adv. Sci.* **2019**, *6*, 1901345.
- [5] D. E. Smalley, Q. Y. J. Smithwick, V. M. B. Jr, J. Barabas, S. Jolly, *Nature* **2013**, *498*, 313.
- [6] H. Chou, W. Huang, *Opt. Lett.* **2020**, *45*, 4543.
- [7] C. Li, M. Xia, Q. Mu, B. Jiang, L. Xuan, Z. Cao, *Opt. Express* **2009**, *17*, 10774.
- [8] I. Kim, W. Kim, K. Kim, M. A. Ansari, M. Q. Mehmood, T. Badloe, Y. Kim, J. Gwak, H. Lee, Y. Kim, J. Rho, *Sci. Adv.* **2021**, *7*, eabe9943.
- [9] T. J. White, D. J. Broer, *Nat. Mater.* **2015**, *14*, 1087.
- [10] S. J. Woltman, G. D. Jay, G. P. Crawford, *Nat. Mater.* **2007**, *6*, 929.
- [11] J. Prakash, A. Parveen, Y. K. Mishra, A. Kaushik, *Biosens. Bioelectron.* **2020**, *168*, 112562.
- [12] J. Sautter, I. Staupe, M. Decker, E. Rusak, D. N. Neshev, I. Brener, Y. S. Kivshar, *ACS Nano* **2015**, *9*, 4308.
- [13] A. Komar, R. P. Dominguez, A. Miroshnichenko, Y. Yu, Y. S. Kivshar, A. I. Kuznetsov, D. Neshev, *ACS Photonics* **2018**, *5*, 1742.
- [14] K. Yin, Z. He, S. T. Wu, *Adv. Opt. Mater.* **2020**, *8*, 2000170.
- [15] S. Li, X. Xu, R. M. Veetil, V. Valuckas, R. P. Dominguez, A. I. Kuznetsov, *Science* **2019**, *364*, 1087.
- [16] P. Chen, L. Ma, W. Hu, Z. Shen, H. K. Bisoyi, S. Wu, S. Ge, Q. Li, Y. Lu, *Nat. Commun.* **2019**, *10*, 2518.
- [17] H. Chen, R. Zhu, J. He, W. Duan, W. Hu, Y. Lu, M. Li, S. Lee, Y. Dong, S. Wu, *Light: Sci. Appl.* **2017**, *6*, e17043.
- [18] D. Yang, S. Wu, *Fundamentals of Liquid Crystal Devices*, Wiley, Chichester, UK **2015**.
- [19] P. Chen, B. Wei, W. Hu, Y. Lu, *Adv. Mater.* **2020**, *32*, 1903665.
- [20] N. V. Tabiryan, S. V. Serak, S. R. Nersisyan, D. E. Roberts, B. Y. Zel-dovich, D. M. Steeves, B. R. Kimball, *Opt. Express* **2016**, *24*, 7091.
- [21] H. K. Bisoyi, A. M. Urbas, Q. Li, *Adv. Opt. Mater.* **2018**, *6*, 1800458.
- [22] L. Wang, X. Lin, W. Hu, G. Shao, P. Chen, L. Liang, B. Jin, P. Wu, H. Qian, Y. Lu, X. Liang, Z. Zheng, Y. Lu, *Light: Sci. Appl.* **2015**, *4*, e253.
- [23] C. Yang, T. Tang, R. Pan, P. Yu, C. Pan, *Appl. Phys. Lett.* **2014**, *104*, 141106.
- [24] Z. Shen, S. Zhou, X. Li, S. Ge, P. Chen, W. Hu, Y. Lu, *Adv. Photonics* **2020**, *2*, 036002.
- [25] J. Lv, Y. Liu, J. Wei, E. Chen, L. Qin, Y. Yu, *Nature* **2016**, *537*, 179.
- [26] W. Feng, D. J. Broer, D. Liu, *Adv. Mater.* **2018**, *30*, 1704970.
- [27] S. S. Lee, J. B. Kim, Y. H. Kim, S. H. Kim, *Sci. Adv.* **2018**, *4*, eaat8276.
- [28] P. Chen, L. Ma, W. Duan, J. Chen, S. Ge, Z. Zhu, M. Tang, R. Xu, W. Gao, T. Li, W. Hu, Y. Lu, *Adv. Mater.* **2018**, *30*, 1705865.
- [29] Y. Liu, W. Chen, J. Tang, X. Xu, P. Chen, C. Ma, W. Zhang, B. Wei, Y. Ming, G. Cui, Y. Zhang, W. Hu, Y. Lu, *Adv. Opt. Mater.* **2021**, *9*, 2001776.
- [30] P. Chen, B. Wei, W. Ji, S. Ge, W. Hu, F. Xu, V. Chigrinov, Y. Lu, *Photonics Res.* **2015**, *3*, 133.
- [31] I. C. Khoo, S. T. Wu, *Optics and Nonlinear Optics of Liquid Crystals*, World Scientific Books, Singapore **1993**.
- [32] C. Wang, A. Tam, C. Meng, M. Tseng, G. Li, H. Kwok, *Opt. Lett.* **2020**, *45*, 5323.
- [33] Q. Dai, Z. Guan, S. Chang, L. Deng, J. Tao, Z. Li, Z. Li, S. Yu, G. Zheng, S. Zhang, *Adv. Funct. Mater.* **2020**, *30*, 2003990.
- [34] L. Deng, J. Deng, Z. Guan, J. Tao, Y. Chen, Y. Yang, D. Zhang, J. Tang, Z. Li, Z. Li, S. Yu, G. Zheng, H. Xu, C. Qiu, S. Zhang, *Light: Sci. Appl.* **2020**, *9*, 101.
- [35] Z. Li, C. Chen, Z. Guan, J. Tao, S. Chang, Q. Dai, Y. Xiao, Y. Cui, Y. Wang, S. Yu, G. Zheng, S. Zhang, *Laser Photonics Rev.* **2020**, *14*, 2000032.
- [36] S. Kirkpatrick, C. D. Gelatt, M. P. Vecchi, *Science* **1983**, *220*, 671.
- [37] V. Chigrinov, S. Pikin, A. Verevochnikov, V. Kozenkov, M. Khazimullin, J. Ho, D. D. Huang, H. S. Kwok, *Phys. Rev. E* **2004**, *69*, 61713.
- [38] J. A. Cox, T. R. Werner, J. C. Lee, S. A. Nelson, J. W. Bergstrom, *Proc. SPIE* **1990**, *1211*, 116.
- [39] D. Wen, J. J. Cadusch, J. Meng, K. B. Crozier, *Adv. Funct. Mater.* **2020**, *30*, 1906415.
- [40] Y. Bao, Y. Yu, H. Xu, C. Guo, J. Li, S. Sun, Z. Zhou, C.-W. Qiu, X. Wang, *Light: Sci. Appl.* **2019**, *8*, 95.
- [41] J. Li, Y. Wang, C. Chen, R. Fu, Z. Zhou, Z. Li, G. Zheng, S. Yu, C. Qiu, S. Zhang, *Adv. Mater.* **2021**, *33*, 2007507.
- [42] J. Guo, T. Wang, B. Quan, H. Zhao, C. Gu, J. Li, X. Wang, G. Situ, Y. Zhang, *Opto-Electron Adv.* **2019**, *2*, 18002901.
- [43] Z. Deng, Q. Tu, Y. Wang, Z. Wang, T. Shi, Z. Feng, X. Qiao, G. Wang, S. Xiao, X. Li, *Adv. Mater.* **2021**, *33*, 2103472.
- [44] Z. Deng, M. Jin, X. Ye, S. Wang, T. Shi, J. Deng, N. Mao, Y. Cao, B. Guan, A. Alu, G. Li, X. Li, *Adv. Funct. Mater.* **2020**, *30*, 1910610.
- [45] S. Wang, Z. Deng, Y. Wang, Q. Zhou, X. Wang, Y. Cao, B. Guan, S. Xiao, X. Li, *Light: Sci. Appl.* **2021**, *10*, 24.